The mechanism of interaction between focused ultrasound and microbubbles in blood-brain barrier opening in mice

Yao-Sheng Tung and Fotios Vlachos
Department of Biomedical Engineering, Columbia University, 351 Engineering Terrace, Mail Code 8904, 1210 Amsterdam Avenue, New York, New York 10027

Jameel A. Feshitan and Mark A. Borden[a)]
Department of Chemical Engineering, Columbia University, Room 801 Mudd, 500 West 120th Street, New York, New York 10027

Elisa E. Konofagou[b)]
Department of Biomedical Engineering, Columbia University, 351 Engineering Terrace, Mail Code 8904, 1210 Amsterdam Avenue, New York, New York 10027

(Received 4 February 2011; revised 12 September 2011; accepted 13 September 2011)

The activation of bubbles by an acoustic field has been shown to temporarily open the blood-brain barrier (BBB), but the trigger cause responsible for the physiological effects involved in the process of BBB opening remains unknown. Here, the trigger cause (i.e., physical mechanism) of the focused ultrasound-induced BBB opening with monodispersed microbubbles is identified. Sixty-seven mice were injected intravenously with bubbles of 1–2, 4–5, or 6–8 μm in diameter and the concentration of 10^7 numbers/ml. The right hippocampus of each mouse was then sonicated using focused ultrasound (1.5 MHz frequency, 100 cycles pulse length, 10 Hz pulse repetition frequency, 1 min duration). Peak-rarefactional pressures of 0.15, 0.30, 0.45, or 0.60 MPa were applied to identify the threshold of BBB opening and inertial cavitation (IC). Our results suggest that the BBB opens with nonlinear bubble oscillation when the bubble diameter is similar to the capillary diameter and with inertial cavitation when it is not. The bubble may thus have to be in contact with the capillary wall to induce BBB opening without IC. BBB opening was shown capable of being induced safely with nonlinear bubble oscillation at the pressure threshold and its volume was highly dependent on both the acoustic pressure and bubble diameter.
 [DOI: 10.1121/1.3646905]

PACS number(s): 43.80.Gx, 43.80.Sh [CCC] Pages: 3059–3067

I. INTRODUCTION

The blood-brain barrier (BBB) is well known as being the main obstacle for successfully delivering drugs into the brain parenchyma. To date, the combination of focused ultrasound (FUS) and microbubbles has been shown to be the most promising approach to achieve a localized BBB opening, without damaging the surrounding tissue.[1,2] Several different aspects of this technique have been investigated. First, BBB opening has been achieved in different animals, including mice,[2] rabbits,[3] rats,[4] monkeys,[5,6] and pigs.[7] Second, different acoustic parameters have been studied. It has been shown that the pulse length can influence the threshold of BBB opening, but no significant difference could be found among various pulse repetition frequencies (PRF) or microbubble concentrations.[8,9] Third, in terms of safety, both long-term (1 and 4 weeks)[10,11] and short-term (30 min and 5 h)[12] studies have been reported indicating a safety window in both cases. Recently, the delivery of certain therapeutic compounds has been successfully enhanced, such as chemotherapeutic drugs for glioblastoma treatment[13] and antibodies for Alzheimer's disease.[14] The spatial deposition pattern of molecules of distinct molecular weights delivered through the BBB has also been established to assess the extent of BBB opening.[15]

Regarding the cellular mechanism of a FUS-induced BBB opening, increasing vesicular transport, channel formation, and a tight junction opening were all reported in capillaries after sonication.[16,17] It has been shown that the permeability of endothelial cells could be enhanced by ultrasound-activated microbubbles.[18] The permeability after BBB opening was also studied and found to increase by at least a 100-fold.[19] During sonication, vasoconstriction was observed and that was followed by BBB opening,[20] which shed light into how the ultrasound-activated microbubbles affect brain vasculature. However, the entire sequence of events and physical mechanism on the microbubble interaction with ultrasound and subsequent cell impact during BBB opening remains to be established.

In order to study the physical effects responsible for BBB opening, a passive cavitation detector (PCD) can be used to acquire the acoustic response stemming from the microbubble and tissue interaction during BBB opening. It has been shown that the BBB could be opened by FUS

[a)]Current address: Department of Mechanical Engineering, 427 UCB, University of Colorado, Boulder, CO 80309.
[b)]Also at: Department of Radiology, Columbia University, 630 W. 168th St., P&S Box 28, New York, NY 10032. Author to whom correspondence should be addressed. Electronic mail: ek2191@columbia.edu

without inertial cavitation at a peak negative pressure 0.29 MPa after craniotomy in rabbits.[21] Previous studies by our group reported *in vivo* transcranial cavitation detection in mice and provided evidence that BBB opening could be induced in the absence of inertial cavitation, at 0.30 MPa.[22,23] We have also shown that the murine skull does not affect the detection of inertial cavitation.[22] The microbubble kinetics were also investigated in the rabbit brain using an ultrasound linear array, and the blood flow and the PRF were found to affect the bubble behavior during BBB opening.[24] However, until now, most studies use commercial microbubbles, which are typically polydispersed, as the agent for inducing BBB opening. Thus, it is difficult to determine the role of the microbubble properties in BBB opening.

The bubble diameter is inversely proportional to the resonance frequency, when all other bubble parameters remain the same. For a bubble constrained in a vessel, regardless of the shell property, the resonance frequency increases when the bubble size decreases.[25,26] For example, when the bubble is confined in a compliant, 10-μm-diameter vessel, its resonance frequency at a diameter of 2, 4, 6, and 8 μm is 3.92, 1.93, 1.41, and 1.26 MHz, respectively.[26] Therefore, the FUS frequency used in this study (1.5 MHz) is close to the resonance frequency of 4–5 μm bubbles. High-speed camera findings have also indicated that the pressure threshold of bubble fragmentation increases with bubble size.[27] Recently, monodispersed microbubbles were shown as an important factor in high-frequency ultrasound imaging.[28] It has also been shown that the pressure threshold of BBB opening is bubble-size dependent. The threshold of 1–2 μm microbubbles was higher than that of 4–5 μm microbubbles,[29] which underlined the importance of the microbubble role in BBB opening. Therefore, the physical mechanism of FUS-induced BBB opening may also be bubble-size dependent, so understanding the role of different microbubble sizes is very important to unveil the physical mechanism of BBB opening.

The objective of this study was to unveil the physical effects of different microbubble sizes responsible for FUS-induced BBB opening. Microbubbles were size-isolated into 1–2, 4–5, and 6–8 μm diameter ranges and the acoustic response of different-sized microbubbles were transcranially detected during BBB opening. The threshold of BBB opening and BBB opening volume at different microbubble sizes was determined by magnetic resonance imaging (MRI). Histological analysis was also performed for damage assessment. Finally, the physical effects of the bubble size responsible for FUS induced BBB opening will be discussed in the discussion section.

II. MATERIALS AND METHODS

A. Monodispersed microbubbles

Lipid-shelled microbubbles with three different diameters (1–2, 4–5, and 6–8 μm) were in-house manufactured and size-isolated using differential centrifugation described in Feshitan *et al.*[30] The concentration was diluted from a higher concentration to approximately 10^7 numbers/ml after microbubble administration and the sonication was performed immediately after microbubble administration. Microbubble size distributions and concentrations were determined by laser light obscuration and scattering (Accusizer 780 A; NICOMP Particle Sizing Systems, Santa Barbara, CA). The number- and volume-weighted size distributions before and after (~8 h later) the experiments (those were unused bubbles obtained from the same vial at those times) are shown in Fig. 1, which also shows that the microbubbles used for BBB opening remain stable. In this study, two sets of 1–2 μm diameter bubbles were found not to be stable after the experiments, i.e., the peak in the number distribution was still 1–2 μm, but the peak in the volume distribution had shifted to a larger diameter (~4–8 μm). However, the results of the two vials were statistically different from the 4–5 and 6–8 μm diameter bubbles, which led to the conclusion that the number distribution is a more reliable measure of stability.

B. Ultrasound

The experimental setup is shown in Fig. 2. A single-element, circular FUS transducer with a hole in its center was driven by a function generator (Agilent Technologies, Palo Alto, CA) through a 50 dB power amplifier (ENI Inc., Rochester, NY). The center frequency, focal depth, outer radius, and inner radius of FUS were 1.5 MHz, 60 mm, 30 mm, and 11.2 mm, respectively. A single-element pulse-echo transducer [center frequency: 10 MHz, focal length: 60 mm (Olympus NDT, Waltham, MA)] was positioned through the center hole of the FUS transducer. The two transducers were aligned so that their focal regions fully overlapped within the confocal volume. A cone filled with degassed and distilled water was mounted on the transducer system.

The PCD transducer, which was connected to a digitizer (Gage Applied Technologies, Inc., Lachine, QC, Canada) through a 20 dB amplification (5800, Olympus NDT, Waltham, MA), was used to passively acquire acoustic emissions from microbubbles with $\pm$ 1 V input range. The pulse length, PRF and the total sonication duration were respectively 100 cycles, i.e., 67 μs, 10 Hz, and 1 min. Prior to the microbubble administration, a 2 s sonication was applied in order to get the baseline of acoustic response used in the quantification of cavitation dose. Peak-rarefactional acoustic pressures of 0.15, 0.30, 0.45, and 0.60 MPa were used in this study. The pressure amplitude was calibrated in degassed water and accounted for 18.1% attenuation through the murine skull.[31] All procedures used on the mice were approved by the Columbia University Institutional Animal Care and Use Committee. Sixty-seven ($n = 67$) adult male mice [strain: C57BL/6, weight: 23.91 $\pm$ 1.56 g (Harlan Sprague Dawley, Indianapolis, IN)] were sonicated. In this study, the right hippocampus was targeted and the left hippocampus served as the control following a precise grid-targeting procedure.[31] The focus was placed 3 mm beneath the skull so that the focal region overlapped with the right hippocampus. The number of mice used at each pressure and bubble size is shown in Table I.

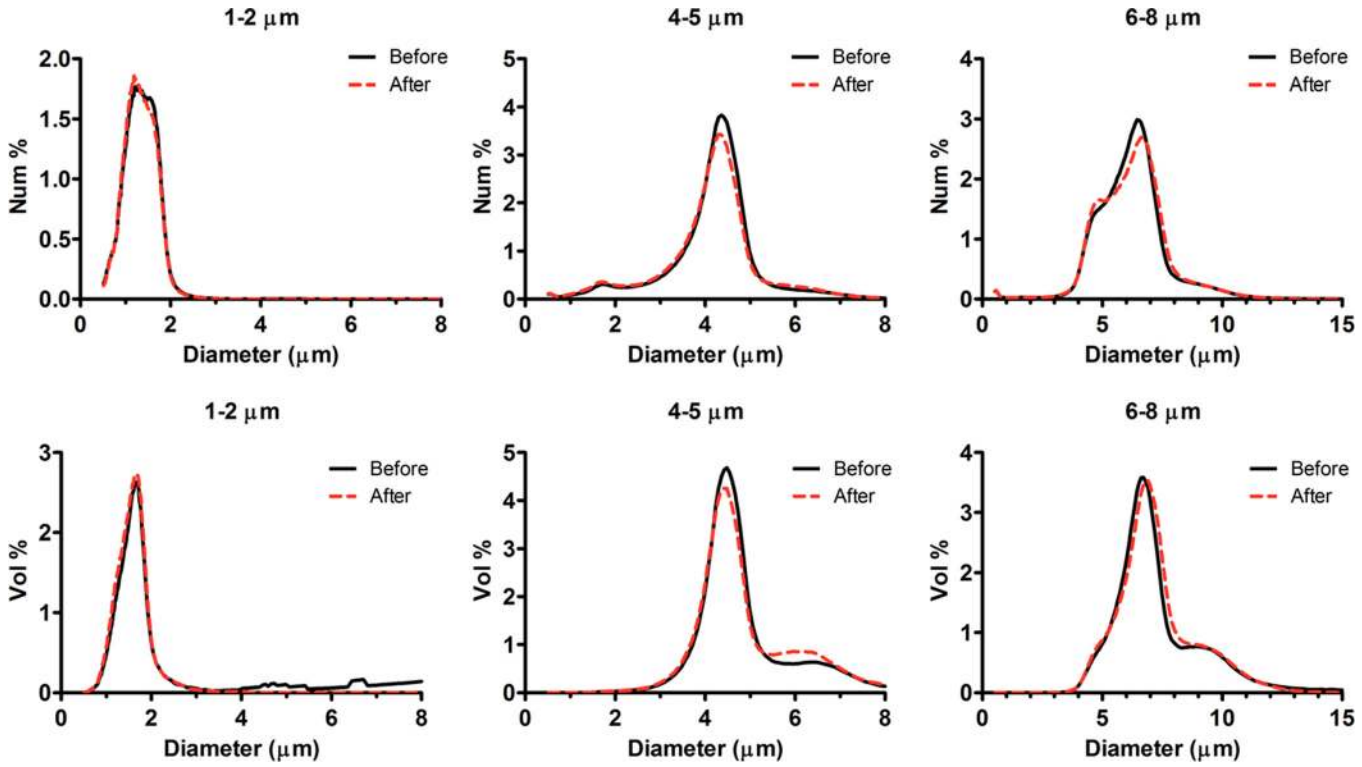

FIG. 1. (Color online) Size distributions of three monodispersed microbubbles are depicted as the number-weighted percent of the total concentration of bubbles and volume-weighted percent of the total volume of bubbles. After microbubbles are manufactured, the distribution is centralized at 1–2, 4–5, and 6–8 μm (solid line). Distribution analysis is performed again on the same day from the same vial, after *in vivo* experiments (dashed line).

C. MRI

A vertical-bore 9.4 T MR system (Bruker Biospin, Billerica, MA) was used to confirm and quantify the BBB opening in the murine hippocampus. Each mouse was anesthetized using 1%–2% of isoflurane gas and positioned inside the single resonator. The respiration rate was monitored throughout the procedure using a monitoring system (SA Instruments Inc., Stonybrook, NY). A two-dimensional FLASH T1-weighted sequence (TR/TE = 230/3.3 ms; flip angle: 70°; NEX = 18; scan time: 9 min 56 s, matrix size: 256 × 192; spatial resolution: 86 × 86 μm^2; slice thickness: 500 μm with no interslice gap) was applied ~50 min after intraperitoneal injection of 0.30 ml of gadodiamide (Omniscan®, GE Healthcare, Princeton, NJ), which allowed sufficient time for the gadodiamide to diffuse into the sonicated region.[19,32] MR imaging was performed 1 h after sonication to confirm the location of the BBB opening.

The volume of BBB opening was quantified using Medical Image Processing, Analysis, and Visualization software (MIPAV, Center for Information Technology, National Institutes of Health, Bethesda, MD). In each 2D horizontal image, an intensity threshold was determined from the left hippocampal region. A level set volume of interest was then used to analyze the intensity values and identify the contour boundary of the BBB opening, where the intensity was higher than a prespecified threshold. After defining the area and the thickness of each slice, the BBB opening volume was calculated.

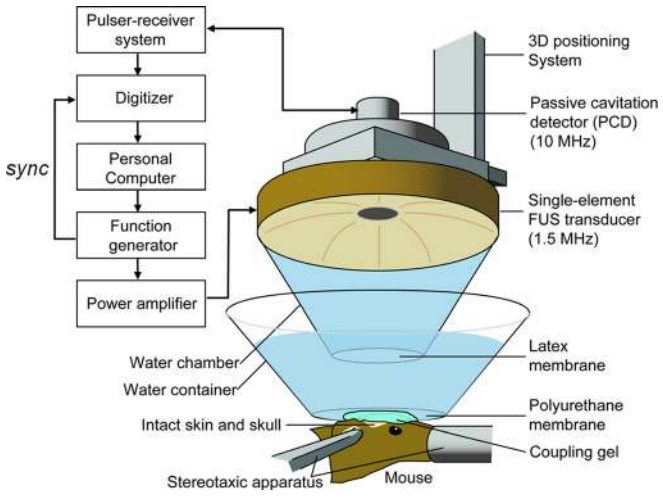

FIG. 2. (Color online) Experimental setup of *in vivo* FUS-induced BBB opening and transcranial cavitation detection. A 10 MHz pulse-echo transducer serves as the passive cavitation detector (PCD) in this study.

TABLE I. Number of mice studied at each pressure and each bubble size.

	Pressure				Total
Diameter (μm)	0.15 MPa	0.30 MPa	0.45 MPa	0.60 MPa	67
1–2	3	6	6	8	23
4–5	4	7	6	6	23
6–8	3	6	5	7	21

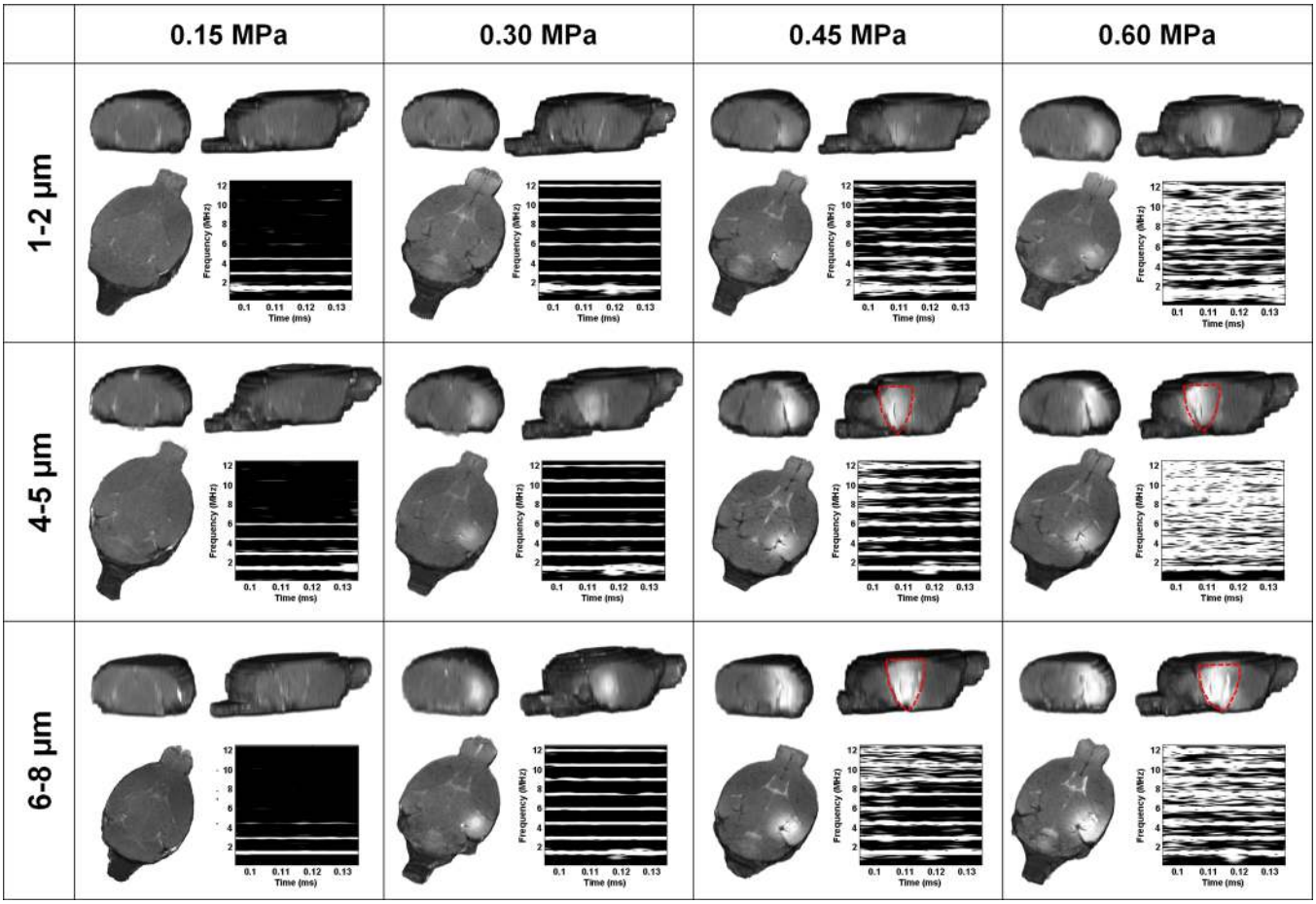

FIG. 3. (Color online) The BBB opening with three bubble diameters confirmed by 3D MRI images with coronal (top left), sagittal (top right), and horizontal (bottom left) views in each table entry. The corresponding spectrogram (bottom right) of the first pulse from 95 to 135 μs with microbubbles administration shows the acoustic response from the microbubbles. In the case of 1–2 μm bubbles, the broadband acoustic emissions are detected at 0.45 and 0.6 MPa, but not at 0.15 and 0.3 MPa. The 3D MR images confirmed that the BBB is opened at 0.45 and 0.60 MPa, with inertial cavitation. In the case of 4–5 and 6–8 μm bubbles, the broadband acoustic emissions are detected at 0.45 and 0.60 MPa, but not at 0.15 and 0.3 MPa. The 3D MR images confirmed that the BBB is opened at 0.30 MPa without inertial cavitation or 0.45 and 0.60 MPa with inertial cavitation. The contour indicates the shielding effects at higher pressures and larger bubbles.

D. Acoustic signal acquisition and analysis

The acoustic emission detected by the PCD was sampled at 100 MHz and a customized spectrogram function (24 cycles, i.e., 16 μs, Chebyshev window; 98% overlap; 4096-point fast Fourier transform) in MATLAB (The MathWorks, Natick, MA) was used to generate a time–frequency spectrograms, which provided the spectral amplitude in time and frequency. The spectrogram can then clearly indicate how the frequency content of a signal changes over time. Therefore, the duration of the broadband response can be demonstrated using the spectrogram.

A high-pass, Chebyshev type 1, filter with a cut-off of 4 MHz was first applied to the acquired PCD signal. In order to remove the harmonic (nf, $n = 1, 2,\ldots,6$), subharmonic ($f/2$) and ultraharmonic ($nf/2$, $n = 3, 5, 7, 9$) frequencies produced by stable cavitation,[33] the response within a 300 kHz bandwidth around each harmonic and 100 kHz bandwidth of each sub- and ultraharmonic frequency were excluded in the inertial cavitation dose (ICD) quantification. These bandwidths were designed to maximize the broadband response bandwidth and to exclude the stable cavitation response in the ICD calculation. The ICD of the spectrogram was defined as the area under the time–amplitude curve over the entire pulse duration.[23,34] After filtering, the time–amplitude curve was obtained from the root-mean-square (rms) of the spectral amplitude at each time point.[23] In order to remove the effect of the skull, the ICD was also calculated without microbubble administration and subtracted from the rms spectral amplitude value with microbubbles to obtain the net bubble response. A Student's t-test was used to determine whether the ICD was statistically different across different pressure amplitudes. A P-value of $P < 0.05$ was considered to denote statistically significant difference in all comparisons.

E. Histology and microscopy

In this study, 55 mice ($n = 55$) were sacrificed 7 days after sonication and 12 mice (one mouse per pressure per bubble size) were sacrificed 3 h after sonication in order to correlate the PCD reading to histological analysis and to study short-term effects. In both cases, the mice were transcardially perfused with 30 ml phosphate-buffered saline for 5 min and then with 60 ml 4% paraformaldehyde for 8 min. Prior to skull removal, the brain was soaked in

paraformaldehyde for one day. Following skull removal, the brain was fixed again in paraformaldehyde for six days. In preparation for paraffin sectioning, the brain was embedded in paraffin and sectioned into 6-μm-thick horizontal sections. 24 out of a total of 72 slices were stained with hematoxylin and eosin (H&E).

III. RESULTS

In this study, only the second harmonic is present at 0.60 MPa in the spectrogram without microbubble administration, which has been shown in our previous study.[23] Therefore, harmonics higher than the third and any broadband response are due to microbubble effects (Fig. 3). The MR images and the corresponding spectrogram of the first pulse *in vivo* are depicted in Fig. 3. Three-dimensional (3D) coronal, sagittal, and horizontal T1-MR images were used to identify the location of BBB opening. As a result of the deposition of the MRI contrast agent induced by BBB opening, the MR images indicate that the threshold of BBB opening is at 0.45 MPa for the 1–2-μm-diameter bubbles and at 0.30 MPa for the 4–5- and 6–8-μm-diameter microbubbles. The corresponding spectrogram shows that only lower harmonics (first to fourth) are detected at 0.15 MPa and higher harmonics (up to eighth) can be detected at 0.30 MPa and beyond at each bubble size. However, the broadband response, i.e., the inertial cavitation, occurs at 0.45 and 0.60 MPa for all microbubbles used in this study. Therefore, BBB opening can be induced by nonlinear oscillation (i.e., with harmonics but without broadband emissions) at 4–5- and 6–8-μm-diameter, but not 1–2-μm-diameter bubbles, at 1.5 MHz excitation frequency.

The ICD, BBB opening volume and their correlation at different bubble diameters are shown in Fig. 4. The ICD at 0.45 and 0.60 MPa is statistically higher than at 0.30 and 0.15 MPa ($P < 0.05$) for all bubble sizes [Fig. 4(a)], which confirms that the threshold of inertial cavitation during BBB opening is ~0.45 MPa. The ICD at 4–5 and 6–8 μm is larger than at 1–2-μm-diameter bubbles ($P < 0.05$) at 0.45 and 0.60 MPa [Fig. 4(b)], which shows that the ICD is also bubble-size dependent. The statistical analysis results of the BBB opening volume at different pressures are shown in Fig. 4(c). The volume at 0.45 and 0.60 MPa is statistically larger than at 0.30 MPa. In the case of the 1–2- and 4–5-μm-diameter bubbles, the volume at 0.60 MPa is statistically larger than at 0.45 MPa (#: $P < 0.05$). The volume with 4–5- and 6–8-μm-diameter bubbles is larger than with 1–2-μm-diameter bubbles (*: $P < 0.05$) at 0.45 and 0.60 MPa [Fig. 4(d)]. In the cases of 0.30 and 0.45 MPa, the BBB opening volume with 6–8 μm is statistically larger than with 4–5-μm-diameter bubbles (#: $P < 0.05$). The correlation between the BBB opening volume and ICD is shown in Fig. 4(e), which shows a linear correlation ($R^2 = 0.85$) when all bubble size and pressures are considered.

Figure 5 shows the histological analysis at the BBB opening threshold at both the 3 h and 7 days time points. In both cases, no cell damage, e.g., red blood cell (RBC) extravasations or dark neurons,[12] was detected after histological examination, which signifies that safe BBB opening can be achieved at all bubble diameters.

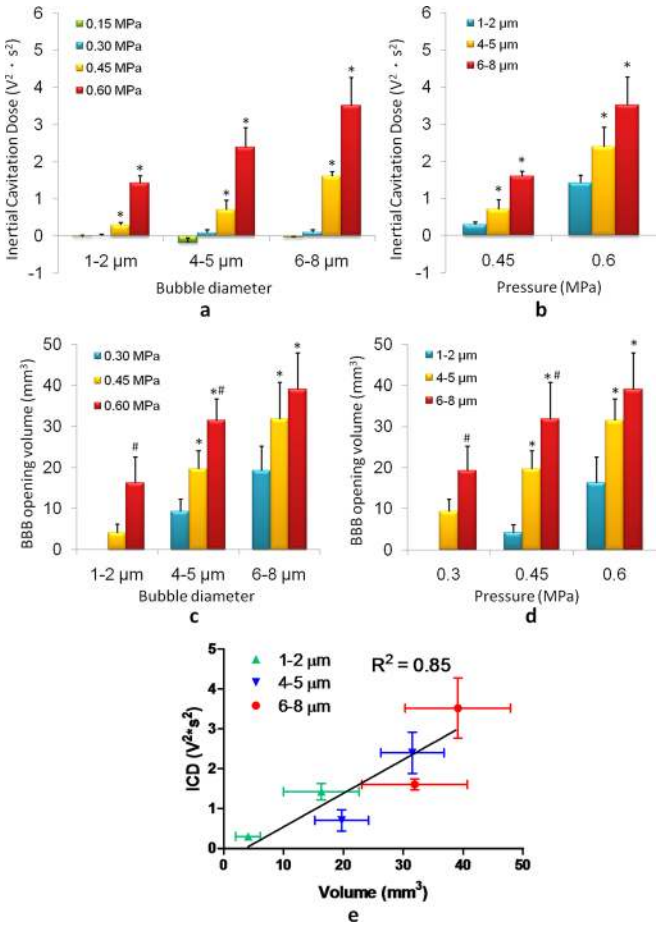

FIG. 4. (Color online) The inertial cavitation dose (ICD) (a) against bubble diameters at four distinct acoustic pressures, and (b) against pressure at three bubble diameters. The ICD at 0.45 and 0.60 MPa are significantly higher than at 0.15 and 0.30 MPa. [*: $P < 0.05$, compared to 0.15 and 0.30 MPa in (a)]. The ICD with 4–5 and 6–8 μm is significantly higher than 1–2 μm at 0.45 and 0.60 MPa. [*: $P < 0.05$, compared to 1–2-μm diameter bubbles in (b)]. The BBB opening volume (c) at three distinct acoustic pressures against the bubble diameter and (d) against pressure at three bubble diameters. It shows that the BBB opening volume is both pressure and bubble-size dependent. [In (c), *: $P < 0.05$, compared to 0.30 MPa. #: $P < 0.05$, compared to 0.45 MPa. In (d), *: $P < 0.05$, compared to 1–2 μm diameter bubbles. #: $P < 0.05$, compared to 4–5 μm diameter bubbles.] (e) Correlation between ICD and BBB opening volume indicated that once inertial cavitation occurs, i.e., pressure is at or above 0.45 MPa, a linear correlation is found between the ICD and BBB opening volume at distinct bubble diameters.

IV. DISCUSSION

The objective of this study was to investigate the physical effects of the systematically circulating microbubbles on the FUS-induced BBB opening. The pressure threshold of BBB opening, determined by the MRI contrast enhancement, was 0.45 MPa for the 1–2 μm and 0.30 MPa for both the 4–5 and 6–8 μm bubbles. However, the spectrogram showed that the broadband response occurred at 0.45 MPa for all microbubbles. The uncorrelated threshold between BBB opening and inertial cavitation implied that the physical effects

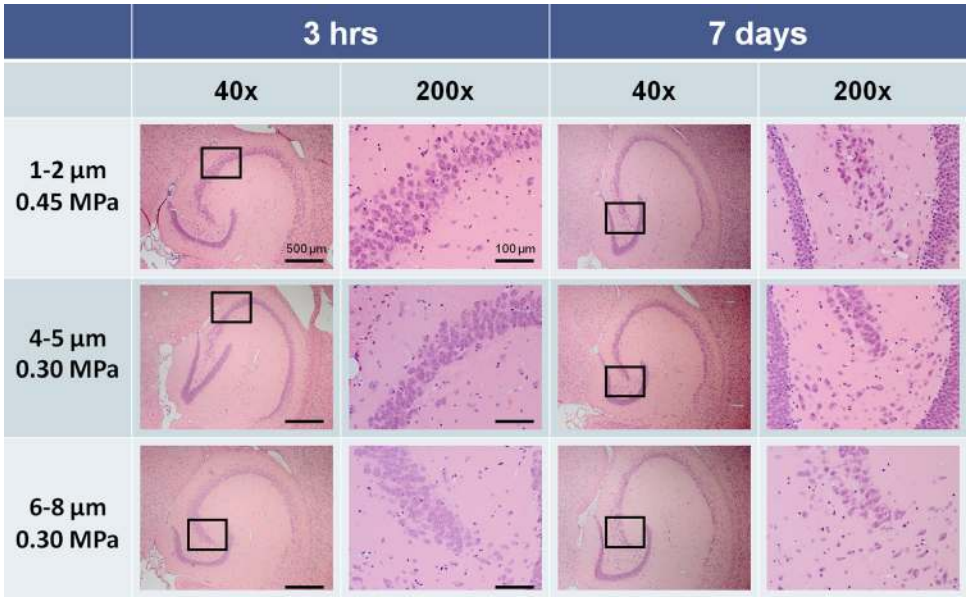

FIG. 5. (Color online) Histology at the BBB opening threshold. The mouse was sacrificed either 3 h or 7 days after sonication. In both cases, no red blood cell extravasations and dark neurons were found with H&E staining, which means that a safe BBB opening can be achieved at the threshold pressure with all bubble diameters.

responsible for the BBB opening may be bubble-size dependent. The inertial cavitation may be necessary for BBB opening with smaller diameter (1–2 μm) but not with larger diameter (4–5 and 6–8 μm) microbubbles.

For larger diameter (4–5 and 6–8 μm) microbubbles, at 0.45 and 0.60 MPa, with the occurrence of inertial cavitation, both the volume and the shape of the contrast enhancement region was different from the case at 0.30 MPa. In the sagittal images, the shape of the contrast enhancement region at 0.45 and 0.60 MPa with 4–5 and 6–8 μm bubbles indicated enhanced shielding effects induced by the bubbles and inertial cavitation occurrence (Fig. 3). However, at 0.30 MPa without inertial cavitation occurrence, the contrast enhancement region, which covered the hippocampal formation [Fig. 6(a)], was more homogeneous and was similar in shape and geometry to the −6 dB focal spot of the FUS beam [Fig. 6(b)].

The capillary diameter in the murine brain ranges between 4 and 8 μm,[35] which is two to eight times larger than the 1–2-μm-diameter bubbles. It has been shown that the microbubble will be fragmented when the radius expands to higher than three times the initial radius at rest (i.e., $R_{max}/R_{rest} > 3$).[36] However, the ratio of expansion of the 4–5- and 6–8-μm-diameter bubbles did not need to be as high as for the 1–2-μm-diameter bubbles to enter into contact with the capillary wall. BBB opening may thus be induced through nonlinear oscillation only in the case of larger bubbles. In addition, the bubbles of 6–8 μm in diameter are even closer in size to the diameter of the capillary, increasing the probability of opening in a larger number of locations. The permeability and reversible BBB opening have been also investigated with different bubble sizes. The BBB opening has also been shown to close within 1–5 days with the same bubble used in this study.[37]

It has been shown that the active vesicular transport is more pronounced in arterioles than in capillaries and venules after BBB opening,[38] which provided evidence that opening is not restricted to the capillaries. As the size of the arterioles was ~10–20 μm,[20] bubble expansion may not be the factor inducing BBB opening in arterioles. According to high-speed photomicrography, localized vessel invagination was observed when the bubble contacted the vessel wall.[39] Vasoconstriction may also be induced by bubble aggregation caused by a secondary radiation force.[20,40] Therefore, larger bubbles may induce vasoconstriction with a higher probability than smaller bubbles. After vasoconstriction is induced by bubble aggregation, the shear stress surrounding the microbubble may be high enough to enhance the permeability of endothelial cells, or to relax the tight junctions. Therefore, the tensile strength of the tight junctions and the shear stress amplitude will be considered in future investigations to determine the physiological effect of FUS-induced BBB opening.

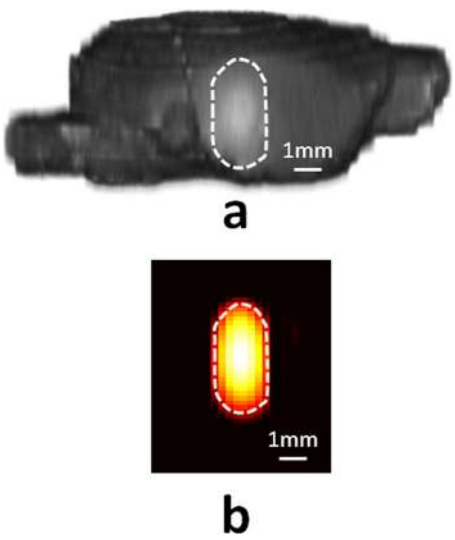

FIG. 6. (Color online) Comparison between (a) the sagittal section of 3D-T1-MR images and (b) −6 dB focal region of the FUS transducer in the case of 6–8 μm bubbles at 0.30 MPa. The consistence between the contrast enhancement region and focal region of the FUS transducer indicates that IC is not necessary to induce a BBB opening.

The spectrogram used in this study clearly elucidated the onset and duration of inertial cavitation within the first pulse. Here, the inertial cavitation occurred at the beginning of sonication. At the highest pressure (0.60 MPa), the broadband response corresponding to the first pulse, lasted throughout the entire duration of the pulse length at all bubble sizes, which indicated that the highest pressure may fragment the microbubbles to smaller bubbles that serve as cavitation nuclei. In the case at 0.15 and 0.30 MPa at all bubble sizes, only harmonics without broadband emissions, were detected. However, the BBB opened at 0.30 MPa only in the 4–5 and 6–8 μm cases. Despite the fact that harmonics up to the eighth could be detected by our PCD, no BBB opening was induced at 0.30 MPa with the 1–2 μm bubbles. Therefore, the nonlinear oscillation of smaller bubbles would not induce BBB opening. The harmonics that corresponded to the nonlinear oscillation of microbubbles may thus not be used as an indicator of BBB opening in the case of the smaller diameter bubbles.

In our previous study, we showed that the BBB was opened at 0.30 MPa using FUS and Definity®.[23] Despite the fact that the mean bubble diameter was within 1.1–3.3 μm, close to 1–2 μm, they were not considered as monodispersed because the maximum diameter was 20 μm and 98% was under 10 μm. It has also been shown that Definity® are polydispersed microbubbles based on the size distribution.[22] Therefore, the BBB opening may be induced by the larger (4–10 μm) bubbles rather than the smaller (1–3 μm) Definity® bubbles at 0.30 MPa.

According to previous reports on Definity® and Optison®, Optison® appeared to produce larger effects than Definity® when applied at the same pressure amplitude with respect to the magnitude of the BBB opening.[41] Here, our findings using both ICD and BBB opening volume confirmed this conclusion. The mean diameter range of Optison® and Definity® was 2.0–4.5 and 1.1–3.3 μm, respectively. Both the effects to the vasculature and the acoustic emission detection were different at distinct microbubble sizes.

Similar to the threshold of BBB opening, the ICD and BBB opening volumes were also bubble-size dependent (Fig. 4). Because of the difference in the scattering cross section, the acoustic emissions increased with the bubble size. Once the bubble rupture occurred, larger bubbles would also induce larger BBB opening volumes. Therefore, a good linear correlation between the ICD and the BBB opening volume was found.

According to the histological analysis at the BBB opening threshold, the BBB opening can be induced without RBC extravasations or neuronal damage (Fig. 5). Despite the fact that the inertial cavitation occurred at 0.45 MPa with the 1–2-μm-diameter bubbles, a small opening volume was induced without any damage. This was consistent with existent sonoporation literature. The intracellular calcium ion concentration ($[Ca^{2+}]$) was changed without being damaged at 0.45 MPa and 1 MHz frequency.[42] In our study, inertial cavitation did not induce cell death, but was sufficient to change the permeability of endothelial cells or rupture the tight junctions.

Standing waves might be generated within a pulse length of 100 cycles. However, based on the spectrograms shown in Fig. 3, no significant change could be observed during the 100-cycle sonication. Also, it has been shown that standing waves were not necessary in the BBB opening mechanism.[43,44] Therefore, the standing wave effect in this study was deemed insignificant.

As mentioned in the materials and methods section, the stability of the 1–2 μm bubbles is being improved in ongoing investigations. During our experiments, monodispersed microbubbles were generated on the same day or 1 day before our experiments. The number-weighted distribution was always centered around 1–2 μm. In every case of the 1–2-μm-diameter bubbles, the BBB was not opened at 0.30 MPa. Therefore, it would also be expected that the threshold of BBB opening might be higher than 0.45 MPa, if the 1–2 μm bubbles are still stable after our experiments.

As the BBB was not opened at 0.15 MPa at all bubble sizes and the diffusion of the gas from the microbubble core will be enhanced in the presence of ultrasound, the discrepancy of the gas volume should not have any impact on the results presented. However, the effect of different gases on the BBB opening should be investigated in the future.

Based on a quantitative summary of findings of this study, the BBB opening pressure threshold, BBB opening volume, inertial cavitation dose, and the percentage of mice with dark neurons are all bubble-size dependent, but the inertial cavitation threshold is not. In this study, the pressure interval was 0.15 MPa, which may not be small enough to determine the real pressure threshold of inertial cavitation. Regarding the neuronal damage, the inertial cavitation with 1–2 μm bubbles can open the BBB without dark neurons, which confirms that the mechanism of BBB opening is also bubble-size dependent. The highest percentage of mice with dark neurons is in the case of 4–5 μm bubbles. As the resonance frequency of 4–5 μm bubbles embedded in a compliant vessel is close to 1.5 MHz,[26] i.e., the FUS frequency used in this study, the inertial cavitation at this bubble size may induce more damage.

V. CONCLUSIONS

The physical mechanism of BBB opening at different bubble sizes was investigated. Inertial cavitation was found to be required for smaller bubbles to induce BBB opening. However, the interaction between larger bubbles and the FUS beam could induce the BBB opening through nonlinear oscillation, without inertial cavitation. No significant damage was detected at the BBB opening threshold, at all bubble sizes. The BBB opening threshold, ICD, and BBB opening volume were found to be bubble-size dependent. Therefore, larger (4–5 and 6–8 μm) diameter bubbles and lower pressure amplitudes (0.20–0.30 MPa) were determined to be safe and consistent in their associated BBB opening.

ACKNOWLEDGMENTS

This study was supported in part by the NIH R01EB009041 and NSF CAREER 0644713. The authors appreciate Keith Yeager, Department of Biomedical Engineering, Columbia University, for manufacturing the cone used in this study. The authors also thank Farbrice Marquet, Ph.D., Jonathan Vaupou, Ph.D., Jianwen Luo, Ph.D., and

Jean Provost, M.S., and Yi Hou, M.S., Department of Biomedical Engineering, Columbia University, for their reliable input.

[1]K. Hynynen, N. McDannold, N. Vykhodtseva, and F. A. Jolesz, "Noninvasive MR imaging-guided focal opening of the blood-brain barrier in rabbits," Radiology **220**, 640–646 (2001).
[2]J. J. Choi, M. Pernot, T. R. Brown, S. A. Small, and E. E. Konofagou, "Spatio-temporal analysis of molecular delivery through the blood-brain barrier using focused ultrasound," Phys. Med. Biol. **52**, 5509–5530 (2007).
[3]K. Hynynen, N. McDannold, H. Martin, F. A. Jolesz, and N. Vykhodtseva, "The threshold for brain damage in rabbits induced by bursts of ultrasound in the presence of an ultrasound contrast agent (Optison)," Ultrasound Med. Biol. **29**, 473–481 (2003).
[4]H. L. Liu, Y. Y. Wai, W. S. Chen, J. C. Chen, P. H. Hsu, X. Y. Wu, W. C. Huang, T. C. Yen, and J. J. Wang, "Hemorrhage detection during focused-ultrasound induced blood-brain-barrier opening by using susceptibility-weighted magnetic resonance imaging," Ultrasound Med. Biol. **34**, 598–606 (2008).
[5]F. Marquet, Y. S. Tung, T. Teichert, V. P. Ferrera, and E. E. Konofagou, "Noninvasive, transient and selective blood-brain barrier opening in non-human primates in vivo," PLoS One **6**, e22598 (2011).
[6]Y. S. Tung, F. Marquet, T. Teichert, V. Ferrera, and E. E. Konofagou, "Feasibility of noninvasive cavitation-guided blood-brain barrier opening using focused ultrasound and microbubbles in nonhuman primates," Appl. Phys. Lett. **98**, 163704 (2011).
[7]F. Xie, M. D. Boska, J. Lof, M. G. Uberti, J. M. Tsutsui, and T. R. Porter, "Effects of transcranial ultrasound and intravenous microbubbles on blood brain barrier permeability in a large animal model," Ultrasound Med. Biol. **34**, 2028–2034 (2008).
[8]J. J. Choi, K. Selert, Z. Gao, G. Samiotaki, B. Baseri, and E. E. Konofagou, "Noninvasive and localized blood-brain barrier disruption using focused ultrasound can be achieved at short pulse lengths and low pulse repetition frequencies," J. Cereb. Blood Flow Metab. **31**, 725–737 (2010).
[9]N. McDannold, N. Vykhodtseva, and K. Hynynen, "Effects of acoustic parameters and ultrasound contrast agent dose on focused-ultrasound induced blood-brain barrier disruption," Ultrasound Med. Biol. **34**, 930–937 (2008).
[10]K. Hynynen, N. McDannold, N. Vykhodtseva, S. Raymond, R. Weissleder, F. A. Jolesz, and N. Sheikov, "Focal disruption of the blood-brain barrier due to 260-kHz ultrasound bursts: a method for molecular imaging and targeted drug delivery," J. Neurosurg. **105**, 445–454 (2006).
[11]N. McDannold, N. Vykhodtseva, S. Raymond, F. A. Jolesz, and K. Hynynen, "MRI-guided targeted blood-brain barrier disruption with focused ultrasound: histological findings in rabbits," Ultrasound Med. Biol. **31**, 1527–1537 (2005).
[12]B. Baseri, J. J. Choi, Y. S. Tung, and E. E. Konofagou. "Multi-modality safety assessment of blood-brain barrier opening using focused ultrasound and definity microbubbles: A short-term study," Ultrasound Med. Biol. **36**, 1445–1459 (2010).
[13]H. L. Liu, M. Y. Hua, P. Y. Chen, P. C. Chu, C. H. Pan, H. W. Yang, C. Y. Huang, J. J. Wang, T. C. Yen, and K. C. Wei, "Blood-brain barrier disruption with focused ultrasound enhances delivery of chemotherapeutic drugs for glioblastoma treatment," Radiology **255**, 415–425 (2010).
[14]J. F. Jordao, C. A. Ayala-Grosso, K. Markham, Y. Huang, R. Chopra, J. McLaurin, K. Hynynen, and I. Aubert, "Antibodies targeted to the brain with image-guided focused ultrasound reduces amyloid-beta plaque load in the TgCRND8 mouse model of Alzheimer's disease," PLoS One **5**, e10549 (2010)
[15]J. J. Choi, S. Wang, Y. S. Tung, B. Morrison III, and E. E. Konofagou, "Molecules of various pharmacologically-relevant sizes can cross the ultrasound-induced blood-brain barrier opening in vivo," Ultrasound Med. Biol. **36**, 58–67 (2010)
[16]N. Sheikov, N. McDannold, N. Vykhodtseva, F. Jolesz, and K. Hynynen, "Cellular mechanisms of the blood-brain barrier opening induced by ultrasound in presence of microbubbles," Ultrasound Med. Biol. **30**, 979–989 (2004).
[17]N. Sheikov, N. McDannold, S. Sharma, and K. Hynynen, "Effect of focused ultrasound applied with an ultrasound contrast agent on the tight junctional integrity of the brain microvascular endothelium," Ultrasound Med. Biol. **34**, 1093–1104 (2008).
[18]K. Kooiman, M. Emmer, M. Foppen-Harteveld, A. van Wamel, and N. de Jong, "Increasing the endothelial layer permeability through ultrasound-activated microbubbles," IEEE Trans. Biomed. Eng. **57**, 29–32 (2010).
[19]F. Vlachos, Y. S. Tung, and E. E. Konofagou, "Permeability assessment of the focused ultrasound-induced blood-brain barrier opening using dynamic contrast-enhanced MRI," Phys. Med. Biol. **55**, 5451–5466 (2010).
[20]S. B. Raymond, J. Skoch, K. Hynynen, and B. J. Bacskai, "Multiphoton imaging of ultrasound/Optison mediated cerebrovascular effects in vivo," J. Cereb. Blood Flow Metab. **27**, 393–403 (2007).
[21]N. McDannold, N. Vykhodtseva, and K. Hynynen, "Targeted disruption of the blood-brain barrier with focused ultrasound: association with cavitation activity," Phys. Med. Biol. **51**, 793–807 (2006).
[22]Y. S. Tung, J. J. Choi, B. Baseri, and E. E. Konofagou, "Identifying the inertial cavitation threshold and skull effects in a vessel phantom using focused ultrasound and microbubbles," Ultrasound Med. Biol. **36**, 840–852 (2010).
[23]Y. S. Tung, F. Vlachos, J. J. Choi, T. Deffieux, K. Selert, and E. E. Konofagou, "In vivo transcranial cavitation threshold detection during ultrasound-induced blood-brain barrier opening in mice," Phys. Med. Biol. **55**, 6141–6155 (2010).
[24]D. E. Goertz, C. Wright, and K. Hynynen, "Contrast agent kinetics in the rabbit brain during exposure to therapeutic ultrasound," Ultrasound Med. Biol. **36**, 916–924 (2010).
[25]E. Sassaroli and K. Hynynen, "Resonance frequency of microbubbles in small blood vessels: a numerical study," Phys. Med. Biol. **50**, 5293–5305 (2005).
[26]S. Qin and K. W. Ferrara, "The natural frequency of nonlinear oscillation of ultrasound contrast agents in microvessels," Ultrasound Med. Biol. **33**, 1140–1148 (2007).
[27]J. E. Chomas, P. Dayton, D. May, and K. Ferrara, "Threshold of fragmentation for ultrasonic contrast agents," J. Biomed. Opt. **6**, 141–150 (2001).
[28]S. Sirsi, J. Feshitan, J. Kwan, S. Homma, and M. Borden, "Effect of microbubble size on fundamental mode high frequency ultrasound imaging in mice," Ultrasound Med. Biol. **36**, 935–948 (2010).
[29]J. J. Choi, J. A. Feshitan, B. Baseri, S. Wang, Y. S. Tung, M. A. Borden, and E. E. Konofagou, "Microbubble-size dependence of focused ultrasound-induced blood-brain barrier opening in mice in vivo," IEEE Trans. Biomed. Eng. **57**, 145–154 (2010).
[30]J. A. Feshitan, C. C. Chen, J. J. Kwan, and M. A. Borden, "Microbubble size isolation by differential centrifugation," J. Colloid. Interface Sci. **329**, 316–324 (2009).
[31]J. J. Choi, M. Pernot, S. A. Small, and E. E. Konofagou, "Noninvasive, transcranial and localized opening of the blood-brain barrier using focused ultrasound in mice," Ultrasound Med. Biol. **33**, 95–104 (2007).
[32]F. Vlachos, Y. S. Tung, and E. Konofagou, "Permeability dependence study of the focused ultrasound-induced blood-brain barrier opening at distinct pressures and microbubble diameters using DCE-MRI," Magn. Reson. Med. **66**, 821–830 (2011).
[33]C. H. Farny, R. G. Holt, and R. A. Roy, "Temporal and spatial detection of HIFU-induced inertial and hot-vapor cavitation with a diagnostic ultrasound system," Ultrasound Med. Biol. **35**, 603–615 (2009).
[34]W. S. Chen, A. A. Brayman, T. J. Matula, L. A. Crum, and M. W. Miller, "The pulse length-dependence of inertial cavitation dose and hemolysis," Ultrasound Med. Biol. **29**, 739–748 (2003).
[35]B. V. Zlokovic, "The blood-brain barrier in health and chronic neurodegenerative disorders," Neuron **57**, 178–201 (2008).
[36]J. E. Chomas, P. Dayton, J. Allen, K. Morgan, and K. W. Ferrara, "Mechanisms of contrast agent destruction," IEEE Trans. Ultrason. Ferroelectr. Freq. Control **48**, 232–248 (2001).
[37]G. Samiotaki, F. Vlachos, Y. S. Tung, and E. E. Konofagou, "A quantitative pressure and microbubble-size dependence study of focused ultrasound-induced blood-brain barrier opening reversibility in vivo using MRI," Magn. Reson. Med. doi:10.1002/mrm. 23063.
[38]N. Sheikov, N. McDannold, F. Jolesz, Y. Z. Zhang, K. Tam, and K. Hynynen, "Brain arterioles show more active vesicular transport of blood-borne tracer molecules than capillaries and venules after focused ultrasound-evoked opening of the blood-brain barrier," Ultrasound Med. Biol. **32**, 1399–1409 (2006).
[39]H. Chen, W. Kreider, A. A. Brayman, M. R. Bailey, and T. J. Matula, "Blood vessel deformations on microsecond time scales by ultrasonic cavitation," Phys. Rev. Lett. **106**, 034301 (2011).
[40]P. Dayton, A. Klibanov, G. Brandenburger, and K. Ferrara, "Acoustic radiation force in vivo: a mechanism to assist targeting of microbubbles," Ultrasound Med. Biol. **25**, 1195–1201 (1999).

[41]N. McDannold, N. Vykhodtseva, and K. Hynynen, "Use of ultrasound pulses combined with Definity for targeted blood-brain barrier disruption: a feasibility study," Ultrasound Med. Biol. **33**, 584–590 (2007).
[42]R. E. Kumon, M. Aehle, D. Sabens, P. Parikh, Y. W. Han, D. Kourennyi, and C. X. Deng, "Spatiotemporal effects of sonoporation measured by real-time calcium imaging," Ultrasound Med. Biol. **35**, 494–506 (2009).
[43]T. Deffieux and E. E. Konofagou, "Numerical study of a simple transcranial focused ultrasound system applied to blood-brain barrier opening," IEEE Trans. Ultrason. Ferroelectr. Freq. Control **57**, 2637–2653 (2010).
[44]M. A. O'Reilly, Y. Huang, and K. Hynynen, "The impact of standing wave effects on transcranial focused ultrasound disruption of the blood-brain barrier in a rat model," Phys. Med. Biol. **55**, 5251–5267 (2010).